Railways Monitoring by Means of Repeated Space-borne SAR Images

Guido Gatti[1], Teng Wang[1,2] and Daniele Perissin[1,3]

1, Dipartimento di Elettronica e Informazione, Politecnico di Milano, Milan, Italy

2, LIESMARS, Wuhan University, Wuhan, China

3, Institute of Earth and Information Science, Chinese University of Hong Kong, Hong Kong, China

Abstract:

High speed railways require very high stability of the structures on which trains run. As a consequence, the area on which a railway has to be built needs to be carefully analyzed. Interferometric Synthetic Aperture Radar (InSAR) data turn out very useful to this aim. In this work we present a time series InSAR analysis along a railway in Shanghai. Several subsidence areas are indentified by means of Quasi Permanent Scatterer Technique. Moreover, we carry out an interferometric coherence analysis, according to the hypothesis of spatial and temporal uniformity of the target. The obtained results pave the way to the development of ad-hoc strategies to monitor such structures with time series InSAR data.

1. INTRODUCTION

In 2005 the high-speed railway system began being built in different locations in China. The planned system consists of four horizontal and four vertical main railways, which will connect the main metropolises in China. Compared with normal ones, high-speed railways require very high stability of the structures on which trains run with speed up to 350km/h. As a consequence, the displacement of railways needs to be carefully monitored. Usually, considering the importance of stability, material and structure of railway basements are designed to be flexible for local slight deformation. In some extreme cases such as the maglev railway in Shanghai, instruments are purposely installed to continuously monitor the railway motion. However, the expenses of conventional deformation survey are not acceptable for railways with more than one thousand kilometres scale. In addition, as reported in [1], more than 80 cities in China are suffering subsidence where the railway passes.

Interferometric Synthetic Aperture (InSAR) data are very useful to solve the problem at hand, since the swath width of spaceborne SAR images (100km in the case of ESA ERS and Envisat) makes it possible to monitor huge areas at a time. Moreover the archives like those acquired by the European Space Agency (ESA) satellites allow recovering historical deformation time series of several years depending on the area location. The Permanent Scatter (PS) technique, developed in Politecnico di Milano in the late 1990s [2], is a well-known method to extract precise ground deformation estimates from interferometric data stacks. Instead of analyzing each pixel of a SAR image, PSInSAR identifies certain artificial or natural point-like stable reflectors (i.e. PS) from long series of interferometric SAR images. On such points it is possible to obtain height estimates with sub-meter accuracy and millimetric terrain motion detection [3, 4]. The application of the PS-InSAR technique in urban areas has been especially studied in the past [5].

In literature some PS case studies along railways can be found (see e.g. [6, 7]). Figure 1 shows the deformation trends detected by the PS technique along a piece of railway in Italy (courtesy of Tele-Rilevamento Europa - T.R.E. srl.). From Figure 1 a subsidence of around 5mm/year is clearly visible around the north part of the railway. In Figure 1, we see also a higher density of PSs in correspondence of three stations of the imaged railway, where the subsidence shows higher rate. For the rest of the imaged railway, the density of targets depends on the orientation of the tracks with respect to the flying path of the sensor and in some parts it is reduced to a few points.

We can then distinguish two cases: in the first one the structural details of the railway and its inclination allow the radar to directly monitor the structure itself, in the other one the stability of tracks can be in first approximation derived by the motion of surrounding targets. In the second case, whenever the surrounding area is extra-urban and thus poor of PSs, two possible research directions are here addressed: 1) improving the target density by considering also partially coherent targets 2) in case

of long linear rail tracks, exploiting the linearity of the structure to enhance the interferometric coherence.

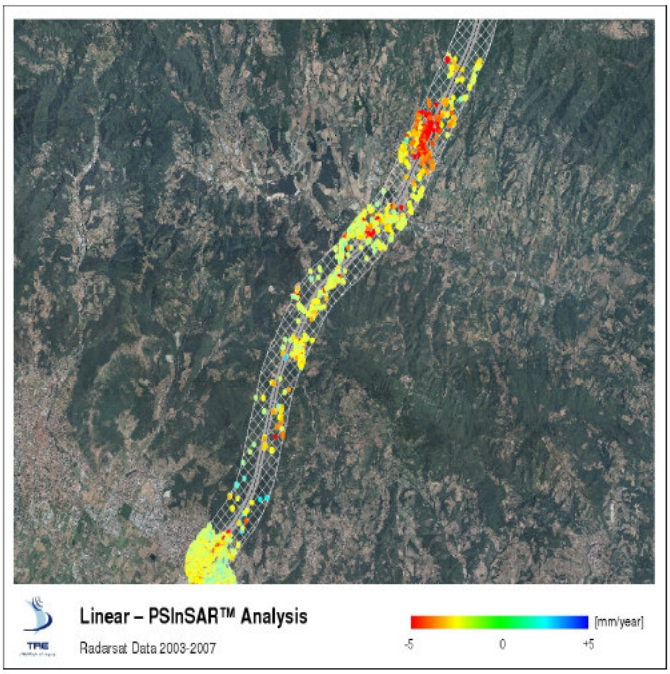

Figure 1 PS analysis along a piece of railway in Italy. Processed by T.R.E. srl

The first research topic held to the development of the Quasi-PS (QPS) technique [8, 9]. The QPS technique allows the identification and exploitation of partially coherent targets to estimate ground motions and terrain elevation where the classical PS technique fails. The second addressed topic deals with InSAR filtering techniques and it assumes that the interferometric phase along the railway is consistent. Thus, by filtering along a linear window, the signal to noise ratio can be enhanced.

In this work we present the time series InSAR analysis results along a straight railway in Shanghai municipality. The railway is observed by 43 ERS-1/2 series of SAR images. Since the railway passes a not urbanized area during the years in which ERS was operative, the QPS technique has been carried out to improve the density of estimated information. Moreover, a one dimension CEW has been used along the railway to separate the signal of the railway from the surrounding noise. The Results presented in this work show the capability of the QPS technique to monitor deformation along railways. In addition, preliminary results of the linear coherence analysis show a good improvement on a subset of interferograms.

2. TEST SITE AND DATA SETS

Shanghai is the largest city in China and one of the largest metropolitan areas in the world, with over 20 million people. Its municipality as a whole consists of a peninsula between the Yangtze and Hangzhou Bay, and the city proper is bisected by the Huangpu River, a branch of the Yangtze River. The vast majority of Shanghai's land area is flat, with an average elevation of 4 meters, and located on an alluvial plain. The particular terrain conformation, together with the over pumping of underground water and the rapid urban development, caused a trend of declining land subsidence in recent years, in which the city sank of several tens of millimetres.

The study area is located in the west part of the municipality of Shanghai. Figure 2 shows the location of the study area and of the railway, which connects the city of Shanghai with the town of Kunshan, passing throw the Jiading district.

On the studied area, 4 different swaths imaged by the radar in 4 different orbits are available. The number of images for each track is shown in Table 1.

Figure 2 Test site in Shanghai

In Figure 3 we show a detail of the reflectivity map (amplitude incoherent mean) of the 4 datasets at hand. Each map represent the same area under different geometries with, at the centre of the scene, a piece of the railway under analysis. From Figure 3 it's evident the dependence of the visibility of the railway with the satellite acquisition geometry: the linear target is clearly visible, with high amplitude values, only in correspondence of the Track 3 dataset.

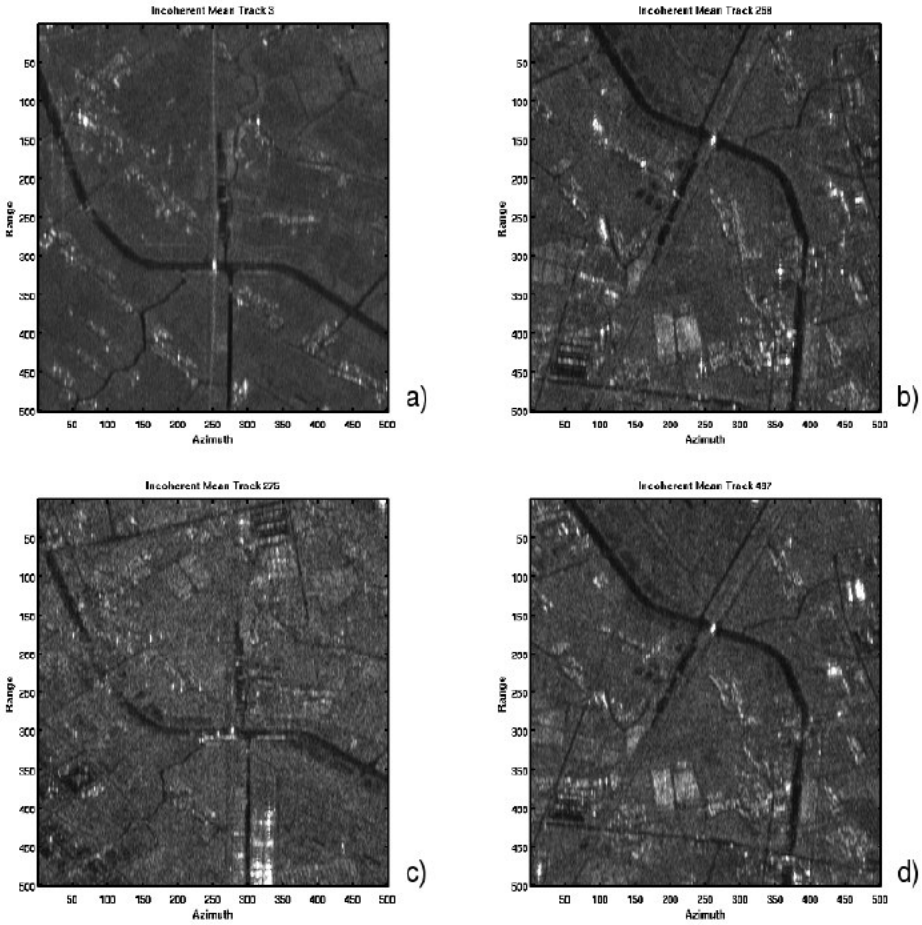

Figure 3 test site in four tracks of ERS time series data sets, namely (a) (b) (c) (d), referred to Track 3, Track 268, Track 275, Track 497.

Table 1 Archived data set in different tracks

Track #	Ascending/Descending	ERS-1 #	ERS-2 #	Envisat#
268	A	-	-	14
497	A	-	-	12
275	D	-	-	9
3	D	17	26	11

Figure 4 shows on the left part another detail of the reflective map of Track 3 centred on a straight stretch of the railway and, on the right side, the amplitude mean calculated along the range direction. It's possible to observe the two amplitude peaks corresponding to the tracks of the railway. In the following we concentrate our attention on the Track 3 dataset.

The dataset under study has been acquired during 1990s. In those years the analyzed area was not urbanized and agricultural fields can be observed from the SAR images. To process the area, we made use of the QPS approach.

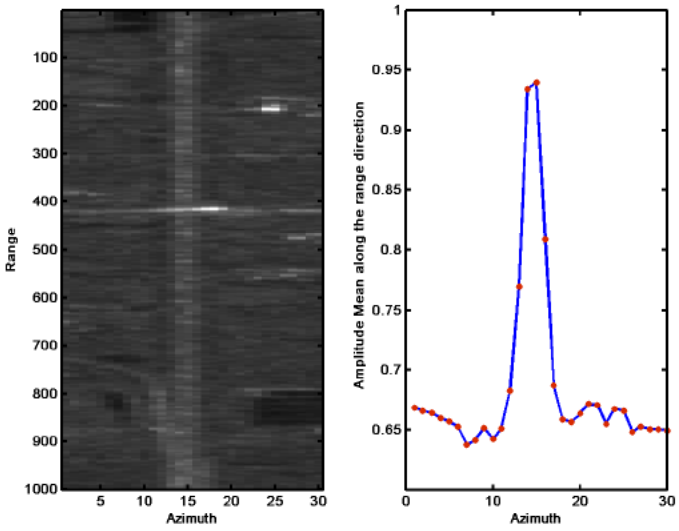

Figure 4 Resample amplitude map over the railway.

3. TIME SERIES INSAR ANALYSIS

Figure 5 collects the main results of the QPS analysis. In the first image on the left, the amplitude map along the railway is shown. For the sake of visualization, the horizontal scale has been magnified by the a factor of 2. Figure 5 (b) shows the PSC candidates selected by analyzing the amplitude series, from which the straight line of the railway can be seen. The temporal coherence estimated by the QPS technique is shown in (c). Although the original PS technique failed to detect coherent targets in this area, by means of the QPS, 5104 points in 20 km^2 with temporal coherence higher than 0.75 were found.

As we mentioned in the previous section, in the 1990s, the test site was still un-urbanized. In fact, comparing Figure 3 (a) with the other 3 reflectivity maps (b,c,d), the bright targets are much fewer. Nevertheless, the density of the detected QPS is still high enough to measure the subsidence of the area. Since the deformation along the railway will be hidden by plotting the estimated deformation trends on all points, only QPS with strong subsidence rates are shown in Figure 5 (d). Along the railway, some abnormal deformation trend can be found on some points. By investigating the test site,

a small train station can be found in the middle of the railway, where some QPS with heavy subsidence are identified. In Figure 5 (e), the subsidence map interpolated with a standard Kriging process along the railway is shown. Areas plotted with red color indicates the detected subsidence. Thus, the time series analysis can offer a good and cheap methods to locate possible risk areas. The result can be used to drive the placement of GPS receivers to study the deformation in time.

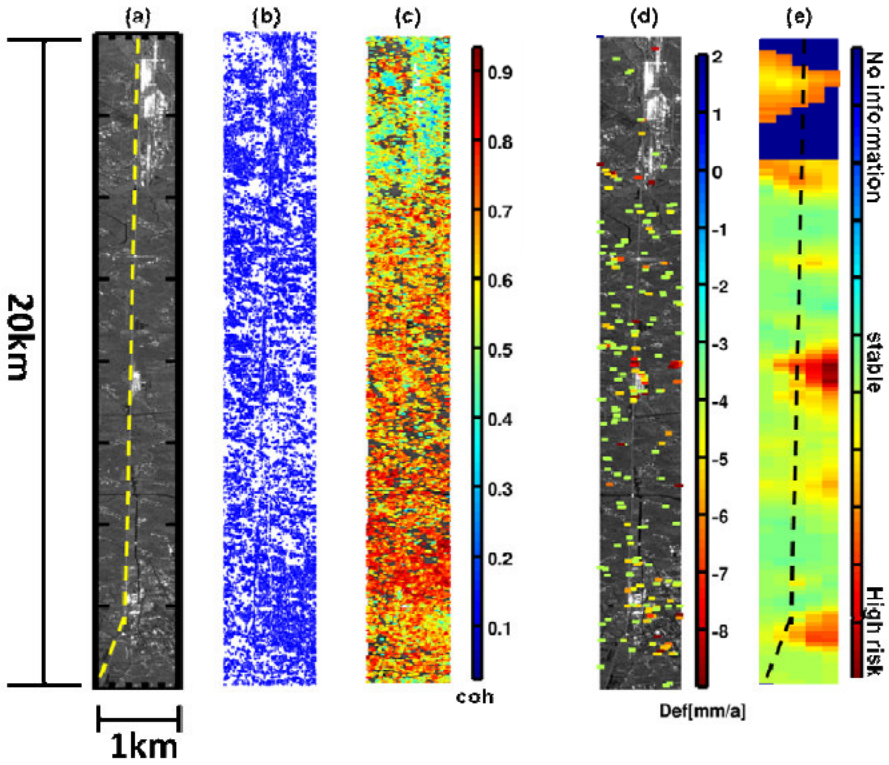

Figure 5 QPS processing results. (a) amplitude map, (b) QPS candidates, (c) temporal coherence, (d) QPS with high subsidence trends (e) Kringing interpolated deformation fields, the red areas indicate high risk subsidence regions along the railway

4. COHERENCE ANALYSIS

A railway is a complicated target formed by a set of different parts like rails, sleepers, poles and the track ballast, but the ensemble of these elementary targets is aligned along the same direction. Thus, a possible model of a railway is that of a uniform and distributed target aligned along a main direction. This hypothesis can be investigated by means of a coherence analysis carried out on the interferogram stacks.

Let us denote with s_i the i-th complex SAR image (with $i, j = 1...N_I$). The interferogram between the images i and j can thus be expressed as $I_{i,j} = s_i \cdot s_j^*$. The spatial coherence $\gamma_p^{i,j}$ of each point p of each interferogram $I_{i,j}$ is retrieved as the normalized cross-correlation coefficient between the two images i,j over an appropriate Coherence Estimation Window $CEW(p)$ [6]:

$$\gamma_p^{i,j} = \frac{\sum_{CEW(p)} I_{i,j}}{\sqrt{\sum_{CEW(p)} |s_i|^2 \sum_{CEW(p)} |s_j|^2}} \quad (1)$$

Within our test site, the straight railway is composed by two different parallel tracks aligned in a direction that differs from the radar slant range direction of an angle less than 1 degree. According to the shape of the railway, a one-pixel wide (4m) CEW is selected, 500m long along the railway direction. In this way, we try to keep separated the two adjacent railway tracks.

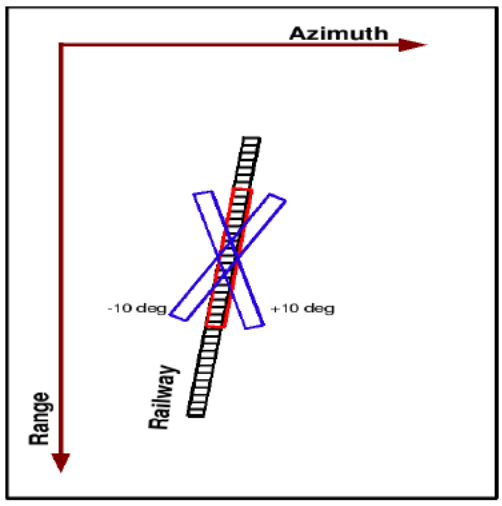

Figure 6 the CEW with different angles. The red one indicated the CEW orientated along the railway.

To highlight the intrinsic coherence of a railway with respect to the surrounding area, it is useful to compare it with the coherence estimated along different directions. In particular, we choose to rotate the CEW angle ϑ between -10 and 10 deg. Given the point p on the railway (with $p = 1...N_p$), we define $\gamma_p^{i,j}(\vartheta)$ as the coherence of the interferogram $I_{i,j}$ along the $CEW(\vartheta)$ centred on point p. Figure 6 displays the geometry of the calculation of $\gamma_p^{i,j}(\vartheta)$ for a point of the railway under different rotations of the estimation window.

As result, we show in Figure 7 the absolute value of the coherence averaged on all the pixels of the railway and with the changing ϑ expressed by:

$$\overline{\gamma}(\vartheta) = \frac{1}{N_{UP(I)}} \frac{1}{N_p} \sum_{\mathrm{UP}(I)} \sum_p \left| \gamma_p^{i,j}(\vartheta) \right| \tag{2}$$

where $UP(I)$ is the upper quartile of the interferograms of the dataset and $N_{UP(I)}$ is the number of $UP(I)$. The result shows how the temporal coherence has the highest value in correspondence of the railway and decreases when we rotate the CEW. According to [11], SAR interferometric coherence can be mainly decomposed into geometric and temporal contributions. Consequently, in the following discussions, the de-correlation of the railway is investigated in these two domains.

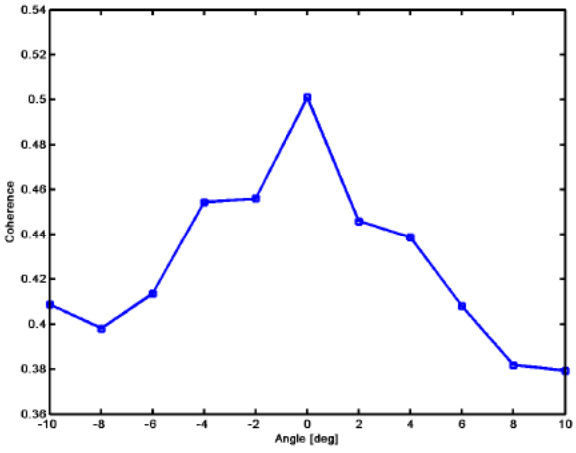

Figure 7 mean coherence estimates with different angles. The highest coherence estimate is obtained along the railway.

4.1 Temporal de-correlation

With our coherence analysis, a covariance matrix [12] is estimated for each pixel along the railway and under different $CEW(\vartheta)$. Since each matrix represents the correlation properties in a particular place in the scene, to resume the coherence of the whole railway compared to the surrounding areas we can average the absolute values of all matrices with respect to a $CEW(\vartheta)$:

$$\overline{\gamma}^{i,j}(\vartheta) = \frac{1}{Np}\sum\nolimits_{p}\left|\gamma_{p}^{i,j}(\vartheta)\right| \tag{3}$$

As a result, we present Figure 8 the averaged covariance matrices for $\vartheta = 0°$ (CEW is aligned with the railway) and $\vartheta = -8°$. The images are arranged by the acquisition date and each element in the matrix represents the coherence of the corresponding interferogram. The principal diagonal is unitary because every image is perfectly coherent with itself.

From the comparison of this two matrices it's easy to notice that there exist a subset of interferograms in which the matrix calculated on $CEW(0°)$ has higher coherence. It is interesting to notice that some of these interferograms also have quite high temporal baselines, instead to be just near the principal diagonal. This extend the de-correlation time of the railway with respect to the surrounding area. Posing a threshold of 0.5, on the railway we can obtain coherent interferograms also between two acquisitions distant 350 days one from each other. On the contrary, in the neighbourhood such coherence is present with temporal baselines of maximum 70 days. This experimental result bears out the hypothesis of high temporal stability of the railway.

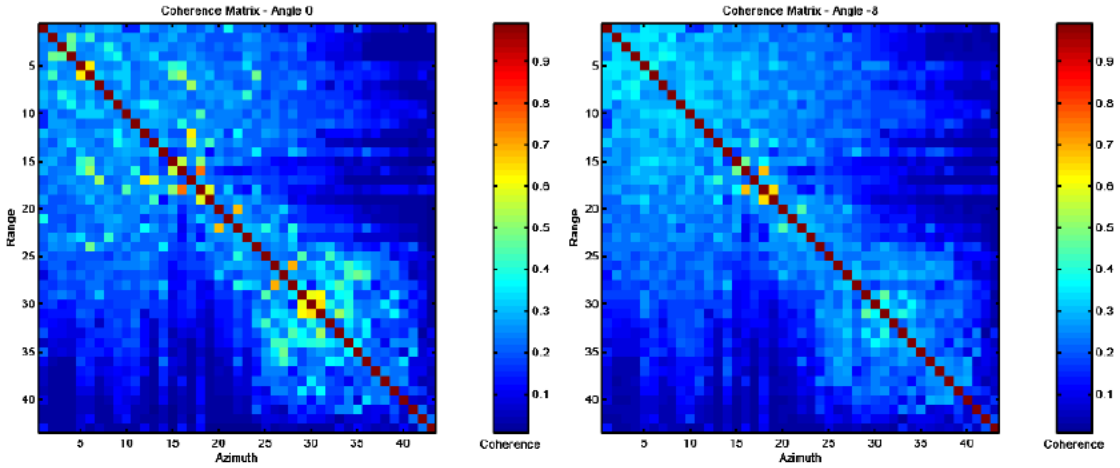

Figure 8 coherence matrices ordered with respect to temporal baselines. (a) calculated on a linear window along the railway, (b) in a different direction.

4.2 Geometric de-correlation

It is of interest looking at the same results of Figure 8 from the normal baseline dimension viewpoint. In Figure 9 the coherence values of the two matrices in Figure 8 are displayed dependent on the normal baseline. The goodness of the interferograms has a strong dependence on this dimension because of the spectral shift that causes a linear-like decrease of the coherence. Moreover it's possible to noticed that values are near to zero with a normal baseline larger than 1000 – 1100 m, which is the ERS critical baseline. This effect, due to the geometric de-correlation, is in agreement with the structure of the railway under analysis, that is not exactly a linear target, but a complicated structure formed of the composition of a set of punctual targets aligned along a main direction.

Also, from Figure 9 we can extract the information of the presence of a subset of interferograms with much higher coherence in correspondence of the railway compared to the surrounding area values. This subset, represented by the outliers from the pseudo-linear distribution, is confined to the low baseline region (smaller than 500m).

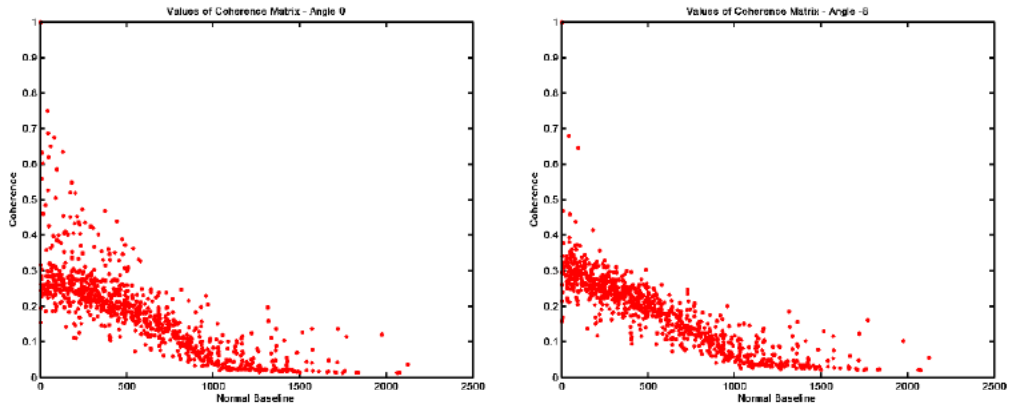

Figure 9 coherence matrices values of Figure 8 ordered with respect to normal baselines. (a) calculated on a linear window along the railway, (b) in a different direction.

5. CONCLUSIONS

Nowadays, China is dedicated in the high-speed railway system construction. By the end of 2009, the railway connecting Wuhan and Guangzhou, with the length of more than 1000km, will be operative. Considering the safety of the running trains, the deformation of such railways has to be monitored precisely and regularly. As a preview work, we present the deformation measures obtained by the QPS technique along a normal railway in Shanghai. From the obtained results, time series InSAR analyses show being able to identify subsiding areas, and consequently offer a good and cheap methods to locate possible risk areas. As a second step, the result can be used to drive the placement of GPS receivers to study the deformation in time. Moreover, since the railway is formed by a set of elementary targets aligned along the same direction, a one-dimensional CEW is proposed and used to exploit the railway by means of a coherence analysis carried out on the interferogram stacks. According to our results, the coherence of the railway keeps high values in long temporal baseline interferograms with respect to the surrounding targets. The proposed linear CEW also improves the spatial coherence estimation and show the potential coherent information along railways. As future work, the same procedures can be used to select the subset of interferograms with highest coherence.

6. ACKNOWLEDGEMENTS

The authors would like to thank ESA for providing the SAR data through ESA-NRSCC Dragon II Cooperation Programme (id 5297) as well as Tele-Rilevamento Europa T.R.E. srl for focusing and registering the SAR data and kindly providing the result shown in Figure 1. Besides, useful discussions with Professor Rocca of Politecnico di Milano are appreciated.

7. REFERENCES

[1] D. Ge, Y. Wang, L. Zhang, Y. Wang, and Q. Hu, "Monitoring urban subsidence with coherent point target SAR interferometry", in Urban Remote Sensing Event, 2009 Joint, 2009, pp. 1-4.

[2] A. Ferretti, C. Prati, and F. Rocca, "Permanent scatterers in SAR interferometry", Geoscience and Remote Sensing, IEEE Transactions on, vol. 39, pp. 8-20, 2001.

[3] A. Ferretti, G. Savio, R. Barzaghi, A. Borghi, S. Musazzi, F. Novali, C. Prati, and F. Rocca, "Submillimeter Accuracy of InSAR Time Series: Experimental Validation", Geoscience and Remote Sensing, IEEE Transactions on, vol. 45, pp. 1142-1153, 2007.

[4] D. Perissin, "Validation of the Sub-metric Accuracy of Vertical Positioning of PS's in C Band", Geoscience and Remote Sensing Letters, IEEE, vol. 5, pp. 502-506, 2008.

[5] D. Perissin, "SAR super-resolution and characterization of urban targets", PhD Thesis, Dipartimento di Elettronica e Informazione, Politecnico di Milano, 2006.

[6] D. Ge, Y. Wang, Xiaofang.Guo, Yi.Wang, and Ye.Xia, "Land Subsidence Investigation Along Railway Using Permanent Scatterers SAR Interferometry", in Geoscience and Remote Sensing Symposium, 2008. IGARSS 2008. IEEE International, 2008, pp. II-1235-II-1238.

[7] Chou Xie, Zhen Li and Xinwu Li, "A Permanent Scatterers Method for Analysis of Deformation over Permafrost Regions of Qinghai-Tibetan Plateau", in Geoscience and Remote Sensing Symposium, 2008. IGARSS 2008. IEEE International, 200, pp. IV-1050-IV-1053.

[8] Perissin, A. Ferretti, R. Piantanida, D. Piccagli, C. Prati, F. Rocca, F. de. Zan. And A. Rucci, "Repeat-pass SAR Interferometry with Partially Coherent Targets", in Fringe07, Frascati, Italy, 2007.

[9] T. Wang, D. Perissin, M. Liao, and F. Rocca, "Deformation Monitoring by Long Term D-InSAR Analysis in Three Gorges Area, China", in Geoscience and Remote Sensing Symposium, 2008. IGARSS 2008. IEEE International, 2008, pp. IV - 5-IV - 8.

[10] R. Touzi, A. Lopes, et al., "Coherence estimation for SAR imagery", Geoscience and Remote Sensing, IEEE Transactions on, vol. 37, pp. 135-149, 1999.

[11] T. Wang, M. Liao, and D. Perrisin, "Coherence Decomposition Analysis", Geoscience and Remote Sensing Letters, IEEE, 2009 (Accepted).

[12] F. Rocca, "Modeling Interferogram Stacks", Geoscience and Remote Sensing, IEEE Transactions on, vol. 45, pp. 3289-3299, 2007.